

ELEVENTH EUROPEAN ROTORCRAFT FORUM

Paper No. 53

THE DEICED SUPER PUMA

J-P. SILVANI

AEROSPATIALE
Helicopter Division
Marignane, France

September 10 - 13, 1985
London, England

THE CITY UNIVERSITY, LONDON, EC1V OHB, ENGLAND.

THE DEICED SUPER PUMA

J-P. SILVANI

AEROSPATIALE, HELICOPTER DIVISION

SUMMARY

The Super-Puma was certificated by DGAC in June 1983 and by FAA in March 1984 for flight in known icing conditions.

The continuous and intermittent icing envelope is that of FAR 23, Appendix C.

The efficiency of protection systems was substantiated through intensive flights in natural icing conditions, icing wind tunnel tests and complementary analysis. The analysis mainly consisted in determining the critical conditions for the claimed icing envelope and showing that the geometrical and thermal dimensioning of rotor protections in these conditions was correct.

The icing wind tunnel tests were intended to develop and validate the air intake and horizontal stabilizer icing protections.

Proper operation of all protections was verified in natural icing flight down to -20°C both in continuous and intermittent icing conditions.

1 - INTRODUCTION

The certification or qualification of helicopters for flight in icing conditions, with or without limitations is covered in the work of a number of helicopter manufacturers.

Flights in natural or simulated icing conditions are an indispensable basis for this process but are not sufficient to provide answers to all the questions concerning the efficiency of the protective systems adopted for a given aircraft against icing. It is in fact virtually impossible to find natural conditions or to simulate conditions which cover all the air-speed, weight, altitude, liquid water content, droplet diameter, temperature parameters which constitute the critical points for which the efficiency of the protection systems must be demonstrated.

Analysis is therefore an indispensable complement to the flights for all certification processes.

The most difficult problem to deal with is the thermal deicing of the blades, in view of the complexity of the aerodynamic flow on the blades and the potential risks (limited efficiency or excessive heating resulting in runback and re-freezing aft of the protected areas) incurred with this type of protection.

AEROSPATIALE has therefore based the certification of the Super-Puma on the flights in natural icing conditions and on the analysis using its own methods or those developed by PAULSTRA and ONERA for the critical points which it was not possible to find during these flights.

In addition to a brief description of the protection systems adopted for the Super-Puma, this paper describes the analysis methods used and their limitations, as well as the main conclusions from the flights in icing conditions.

2 - DESCRIPTION OF THE ICING PROTECTION EQUIPMENT

The table in Figure 1 presents the ice protection equipment for the different Super-Puma components. Their location on the aircraft is shown in Figure 2.

SYSTEMES	PROTECTION SYSTEM
ENGINE AND AIR INTAKE	SCREENS
MAIN ROTOR BLADE LEADING EDGE	ELECTRICAL CYCLIC DEICING
TAIL ROTOR BLADE LEADING EDGE	ELECTRICAL ANTI-ICING
PILOT AND COPILOT FRONT WINDSHIELD	ELECTRICAL HEATING ANTI-ICING
AIR DATA SYSTEM	
♦ TOTAL PRESSURE HEADS	ELECTRICAL ANTI-ICING
♦ STATIC PRESSURE PARTS	NONE
HORIZONTAL STABILIZER	PNEUMATIC CYCLIC DEICING
FUEL TANK AIR VENT	NONE
FUEL DRAIN	NONE
ENGINE COWLING AERATION	NONE
M.G.B. OIL COOLING UNIT	NONE
I.G.B. COOLING UNIT	NONE
HINGE LUBRICATION OIL TANK AIR VENT	NONE
RADOME	NONE
ANTENNAS	NONE
RETRACTING LANDING GEAR	NONE
MAIN ROTOR DROOP RESTRAINTERS	FAIRING
OPTIONAL EQUIPMENT	NONE
ICE DETECTOR	ANTI-ICING USING ELECTRICAL AND P2 AIR HEATING

Fig. 1 : AS 332 ICE PROTECTION SYSTEMS

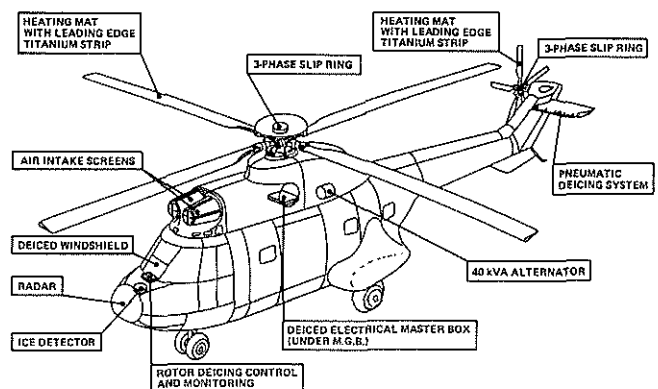


Fig. 2 : LAYOUT OF ICE PROTECTION SYSTEMS

It should be noted that the basic aircraft is already fitted with the following protection systems against unknown icing and associated conditions. These systems are :

- Air intake screens,
- Pitot head anti-icing system,
- Pilot's and copilot's windshield anti-icing systems,
- Lightning protection for the rotors, fuel tanks and fuel tank air vents.

- The main rotor blades are deiced electrically (Figures 3 - 4 - 5). The deicer is made up of 5 resistors incorporated in a glass cloth-reinforced rubber mat. The outside surface is protected against erosion by a titanium sheet.

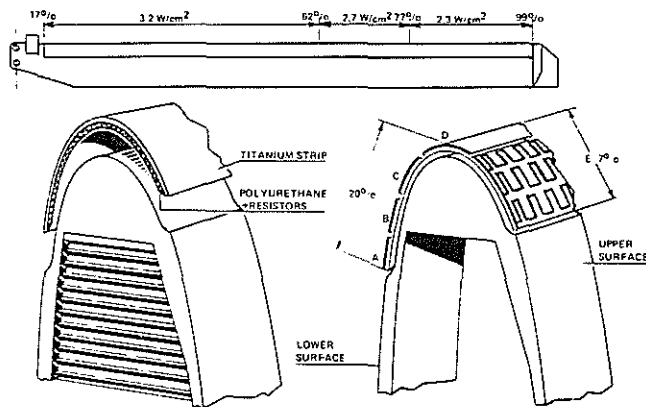


Fig. 3 : SA 330 AND AS 332 DEICED MAIN ROTOR BLADE

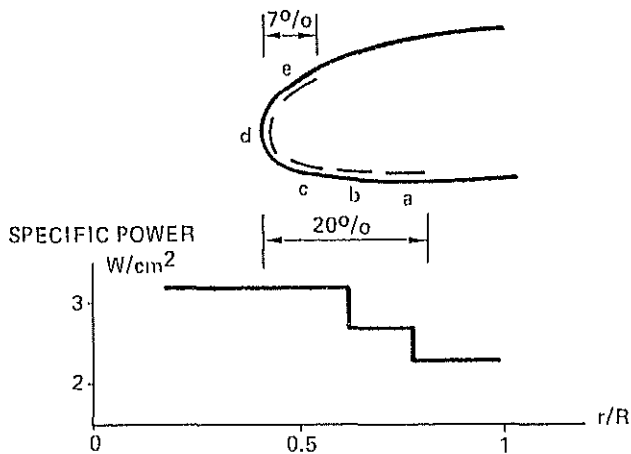


Fig. 4 : DEICER POWER DISTRIBUTION

TEMPERATURE -- 10° C		TEMPERATURE -- 10° C	
d-e-c-b-a		d-e-c-b-d	
WORKING TIME	10 SEC		16 SEC
TIME	43		67
TOTAL	93		147
d-e-c		d-e-c	
WORKING TIME	10		16
TIME	23		35
TOTAL	53		83

Fig. 5 : DEICING SEQUENCE ON AS 332 MAIN ROTOR BLADE

- The tail rotor blades are anti-iced electrically (Figure 6) by means of 3 resistors embedded in the glass cloth and also protected by a titanium sheet.

The rotors are deiced and anti-iced by a redundant electronic assembly which includes electric power sources, control and monitoring modules and slip rings.

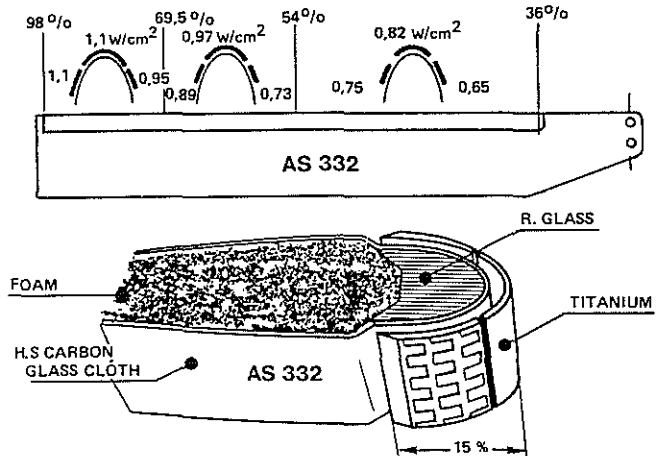


Fig. 6 : AS 332 ANTI-ICED TAIL ROTOR BLADE

- The horizontal stabilizer is deiced pneumatically (Figure 7).

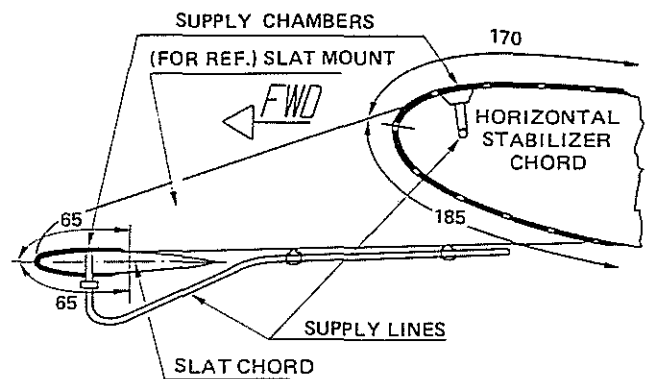


Fig. 7 : AS 332 HORIZONTAL STABILIZER PNEUMATIC DEICING

- The engines are protected against the ingress of ice by unheated screens which also ensure protection against birds, hail stones, etc

As an alternative, the engines may be protected by multi-purpose air intakes of the same type as those for the SA 330 Puma.

3 – DIMENSIONING OF THE ROTOR PROTECTION SYSTEMS

The rotor protection systems were dimensioned empirically on the Puma and extended to the Super-Puma. Analysis conducted a posteriori for the most critical flight situations has shown the effectivity of the solutions adopted.

3.1 – GEOMETRICAL DIMENSIONING OF THE ROTOR PROTECTION SYSTEMS

The assessment of maximum extent of ice accretion on the blades begins with the selection of the most severe cases experienced within the flight envelope. In this envelope, three major parameters may be distinguished :

- Aircraft weight
- Aircraft speed
- Altitude.

After investigating combinations of these three parameters, the maximum weight and speed values for various altitudes specified in the Flight Manual were adopted as the least favourable conditions.

For any calculation of ice accretion, knowledge of the airspeed and incidence of the airflow, to which the airfoils are subjected during a full rotation of the blade, is necessary. These aerodynamic values are used as infinite upstream conditions for calculating the droplet trajectories.

The aim of aerodynamic calculations is to determine, mainly in level flight, the speed and angle of attack for each point of the blade.

During a blade rotation the pair of values : angle of attack (i), Mach (M) follow a curve, called angle of attack-Mach loop. Examples of such loops are given in Figure 8 for the main rotor and Figure 9 for the tail rotor.

When the airspeed and angle of attack are known for each radius and azimuth position on the rotor disc, droplets trajectories can be calculated.

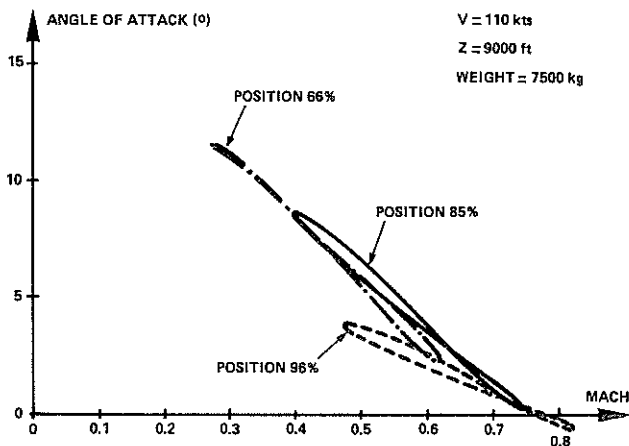


Fig. 8 : ANGLE OF ATTACK/AIRSPEED LOOPS
AS 332 MAIN ROTOR

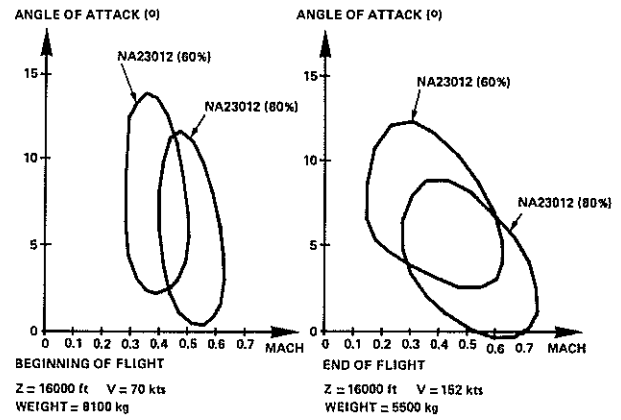


Fig. 9 : ANGLE OF ATTACK/AIRSPEED LOOPS
TAIL ROTOR AS 332

Calculation of droplet trajectories consists in a clear resolution of the dynamic equation ($F = m \times \gamma$) applied to a droplet falling forward of the airfoil. The only noticeable force acting on the droplet is its aerodynamic drag. This force is calculated from the difference between the droplet speed and the local speed of flow. When well forward of the airfoil, the droplet trajectory naturally merges into a flow current line. In the vicinity of the airfoil, the airstreams are subjected to considerable curvature. Owing to its inertia, the droplet then follows a trajectory that differs from the current lines and may strike the airfoil.

An example of thorough calculation is given in Figure 10 for 27 micron diameter droplets.

AS 332 SA 13112 (66%R) HIGH POINT OF I/M LOOP

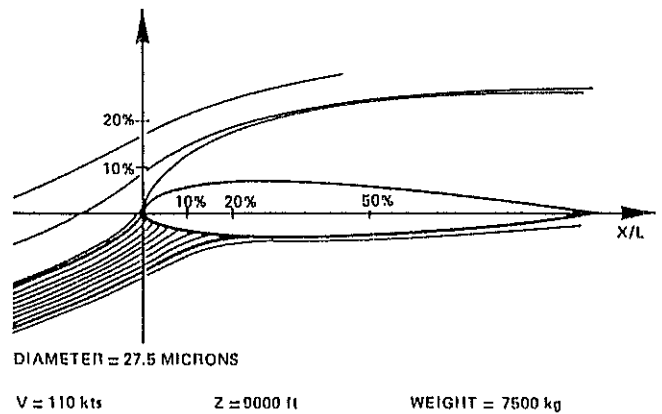


Fig. 10 : DROPLET TRAJECTORIES CALCULATION

A basic parameter of droplet impingement is the accretion coefficient, defined as the ratio of the distance between two adjacent droplets to their distance impact on the airfoil. Figure 11 shows, for the same calculation, the accretion coefficient versus the chordwise position.

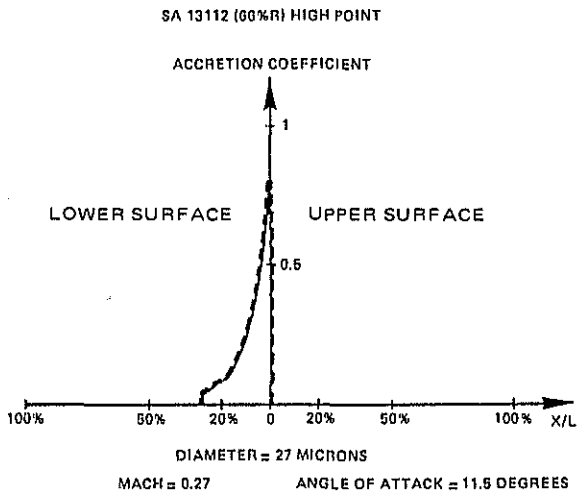


Fig. 11 : ACCRETION COEFFICIENT

When this calculation method is applied to helicopter airfoils, with variable incidence, it substantially confirms the measurements, except for high incidence angles when the theory indicates greater ice accretion on the airfoil lower surface than in reality (Figure 12).

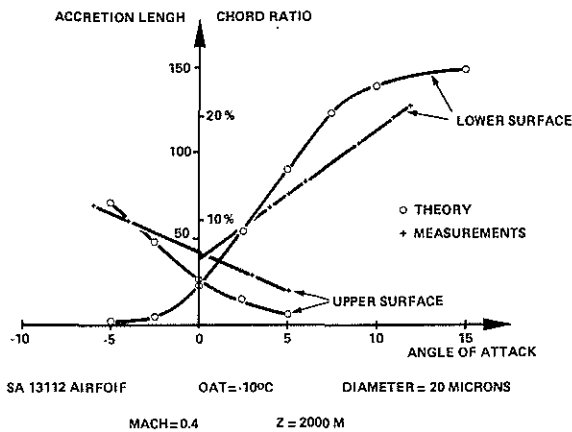


Fig. 12 : COMPARISON BETWEEN THEORY AND WIND TUNNEL MEASUREMENTS

In short, all the calculations carried out under the least favourable incidence and airspeed conditions show that the geometrical dimensioning of the blade protection systems is correct throughout the Super-Puma flight envelope.

3.2 - CALCULATION OF TEMPERATURE DISTRIBUTION IN THE MAIN ROTOR BLADES

3.2.1 - Uni-Directional Calculations

In the calculation program used, heat exchanges are considered only along an axis perpendicular to the surface.

The deicer is divided into sections with a surface area of 1 and the calculation is carried out along the axis which passes through the centre of this surface area.

The deicer is broken down into quite thin layers of homogeneous material (Figure 13).

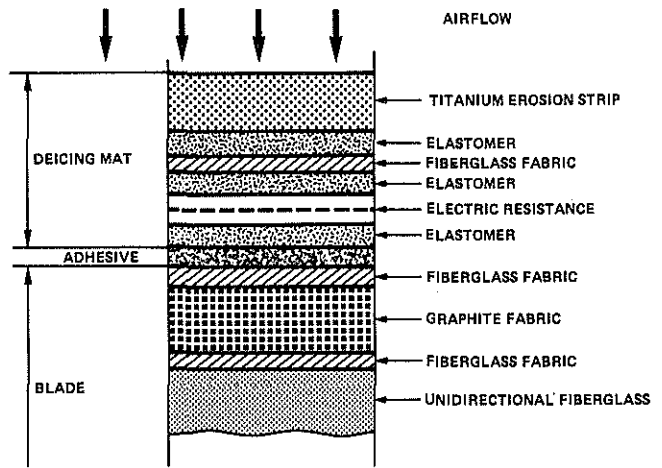


Fig. 13 : UNIDIRECTIONAL LAYOUT OF DEICING MAT

The thickness of ice accumulated on the airfoil is considered in the calculations which were validated by confirmation with measurements in flight or in a wind tunnel on blade sections, in dry air or in icing conditions (Figures 14 and 15).

COMPARISON BETWEEN TESTS AND THEORY - DRY AIR

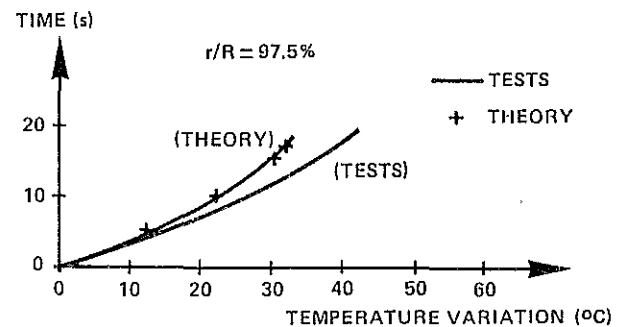
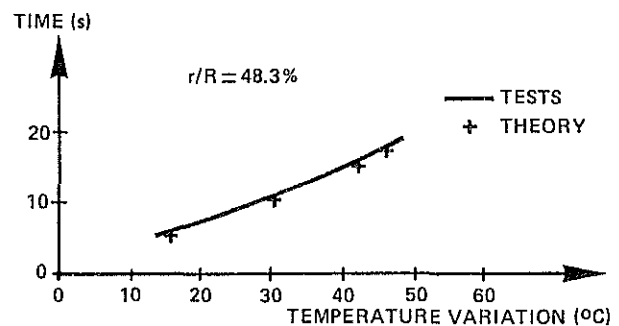
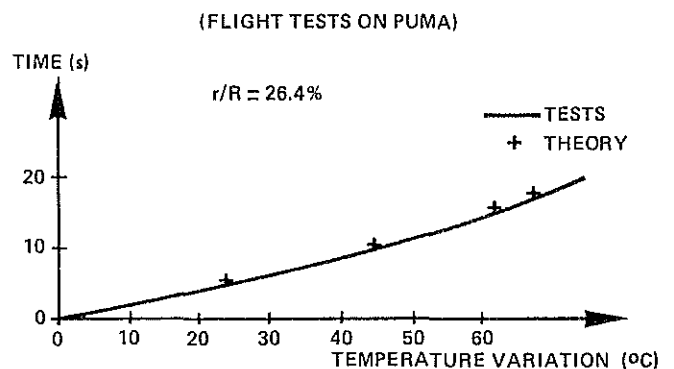


Fig. 14 : TEMPERATURES AT DEICING MAT/BLADE INTERFACE

COMPARISON BETWEEN TESTS AND THEORY – DRY AIR
(FLIGHT TESTS ON PUMA)

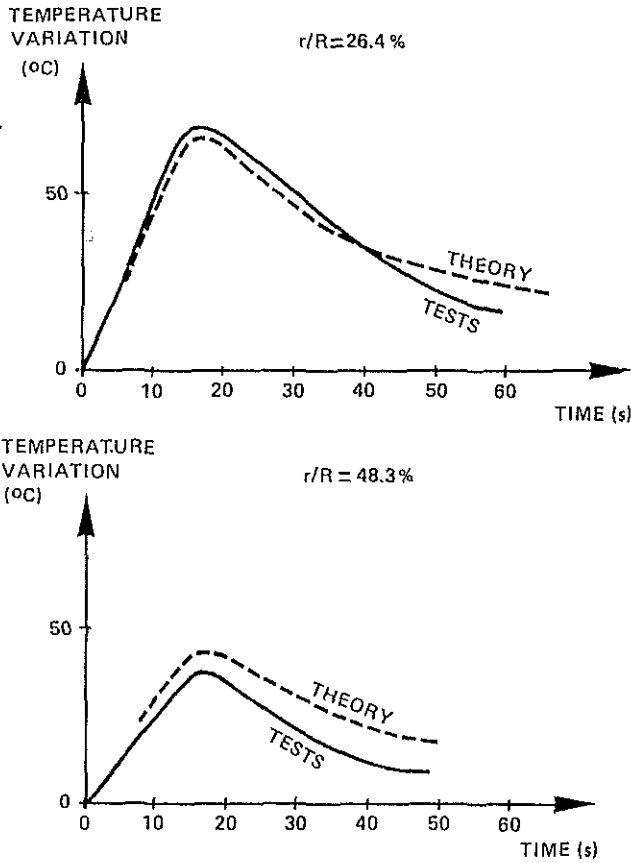


Fig. 15 : TEMPERATURES AT DEICING MAT/ BLADE INTERFACE

Assuming that the ice separates from the deicer when the temperature at the ice-deicer interface reaches $+ 7^{\circ}\text{C}$ (Ref. 1), the calculation shows that the blade deicing is efficient throughout the temperature range down to $- 30^{\circ}\text{C}$ and in particular that the change in the strip heating cycle at $- 10^{\circ}\text{C}$ is justified. (Figure 16)

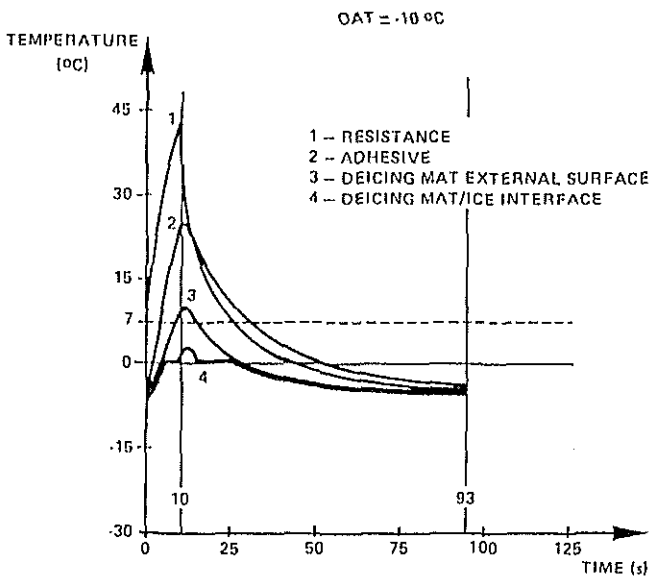


Fig. 16 : TEMPERATURE DISTRIBUTION CALCULATION ON A DEICING MAT

3.2.2 – Bidimensional Calculations

The calculation method used was developed by ONERA.

The airfoil is divided into meshes (Figure 17) whose dimensions are adapted to the material and to the local heating. The bidirectional calculation program resolves the heat conduction equation by the finite element method.

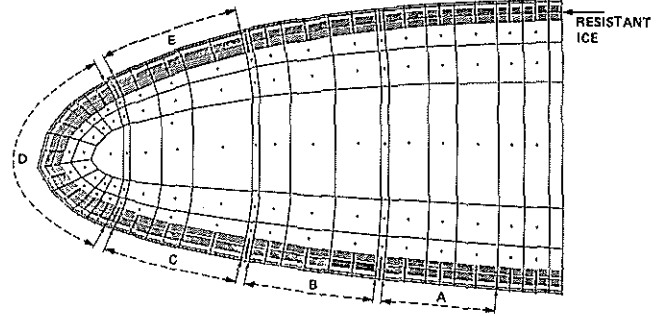


Fig. 17 : ELECTRICAL DEICER CODE – BLADE MODELISATION

Two possibilities were considered for the heat exchange coefficient at the wall :

- in dry air, the heat exchange coefficient is convective. It is determined from the local friction coefficient which is obtained by compressible aerodynamic flow and boundary layer calculations.
- in the presence of ice, the convective heat exchange coefficient is applied to the outside surface of the ice which is modeled as a supplementary material.

As for the unidirectional calculation, the calculations correctly confirm the temperature measurements in flight or in a wind tunnel.

The deicing is taken to be efficient when the ice-deicer interface temperature is equal to or greater than 0°C .

The calculations show that, with the above assumption, the deicing is effective, except at $- 30^{\circ}\text{C}$ (Figure 18). At this temperature, allowing for the adherence of the ice on an eroded surface (Figure 19), the deicer surface temperatures are such that the ice is evacuated naturally by centrifugal effect.

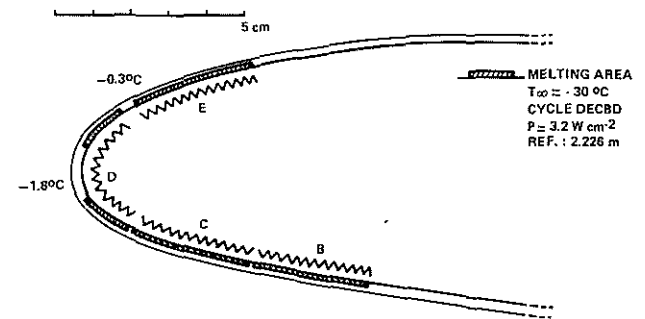


Fig. 18 : ELECTRICAL DEICER CODE – DEICING EFFICIENCY

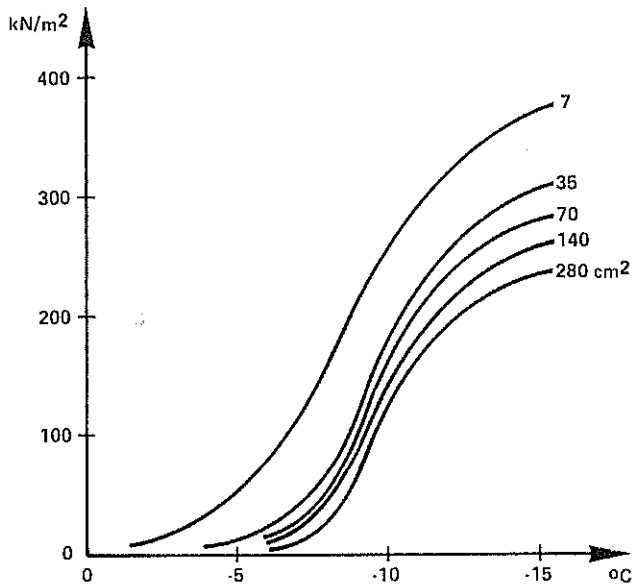


Fig. 19 : SHEDDING STRESS VALUES ACCORDING TO TEMPERATURE AND TO ICED AREA

3.3 – EFFICIENCY OF THE TAIL ROTOR ANTI-ICING SYSTEM

The efficiency of the anti-icing system has been demonstrated by extrapolation of the different surface temperature measurements taken in flight or in a wind tunnel.

Analysis by calculation is not adopted for the anti-icing system since, in view of the fact that the temperatures are stabilized only after several minutes, the difference between the calculated and measured temperatures becomes too great. (Figure 15 shows a significant difference between measured and calculated values after one minute).

4 – SUBSTANTIATION OF THE EFFICIENCY OF THE PROTECTION SYSTEMS IN AN ICING WIND TUNNEL

4.1 – ENGINE AIR INTAKES

The air intake screens which are fitted as aircraft basic equipment items are designed to protect the engines against the ingress of foreign matter and to enable flight in icing conditions without limitations.

The grid performance and efficiency have been confirmed by tests in simulated icing conditions at the Saclay CEP_r facility.

As a whole, the air intake and engine simulated icing tests (Figure 20) showed that the screens protected the engine effectively with acceptable clogging and that the surging margins were conserved.

It should be noted that the most important ice accretion resulting in the highest pressure losses in the air intake was obtained at $-5^{\circ}C$, both at take off and at cruising flight power ratings. Under these flight conditions, the pressure loss due to clogging results in a power reduction of approximately 6 % at the same gas generator speed.

TEST CONDITIONS						
TEST No	Hp (m x 1000) IAS (km/h)	OAT DROPLET DIA (μm)	INCIDENCE ($^{\circ}$)	DURATION (mm) LWC (g/m ³) TYPE	NG (%)	MAX. PRESS. LOSS (%)
1	1.2 265	-5 20	-5	30 0.7/2.4 AI	93.5 93.5	4.7 4.7
2	1.2 265	-5 20	-5	30 0.7/2.4 AI	93.5	1.5
3	1.2 265	-5 30	-5	30 0.4/1.2 AI	93.5	3.7
4	1.2 265	-10 20	-5	30 0.6/2.2 AI	93.5	2.6
5	3.9 130	-30 20	-5	30 0.2/1 AI	99	2
6	1.2 130	-5 20	-5	30 0.7/4.4 AI	83.5	0.9
7	0.3 MINI	-2 30	-5	30 0.6	78	0.8
9	0.3 MINI	-5 25	-5	10 2 IMI	100	5.9 (MEAN VALUE)
11 (CLIMB)	1.2 TO 3.6 130	-5 TO -20 20	-12	IMI	100	3.3
13 (DESCENT)	3.1 TO 1.2 130	-20 TO -5 20	11	IMI	75	1.3
14	3.9 265	-5 20	30 -5	0.7/2.4 AI	99	4.9

AI: ALTERNATE ICING
IMI: INTERMITTENT MAXIMUM ICING

Fig. 20 : AIR INTAKE ICING SUBSTANTIATION TESTS CONDUCTED AT THE CEP_r

4.2 – HORIZONTAL STABILIZER

The necessity to protect the horizontal stabilizer against icing was demonstrated by flight tests with modelled ice forms. These ice forms were obtained in an icing wind tunnel at the Saclay CEP_r facility (Figures 21 and 22). The flights were conducted with 50 and 100 mm ice thickness. Even though the limit stress values on the stabilizer were not exceeded, the deterioration of flying qualities and the increase in the vibratory level above 80 kts were such that the horizontal stabilizer protection proved to be necessary.

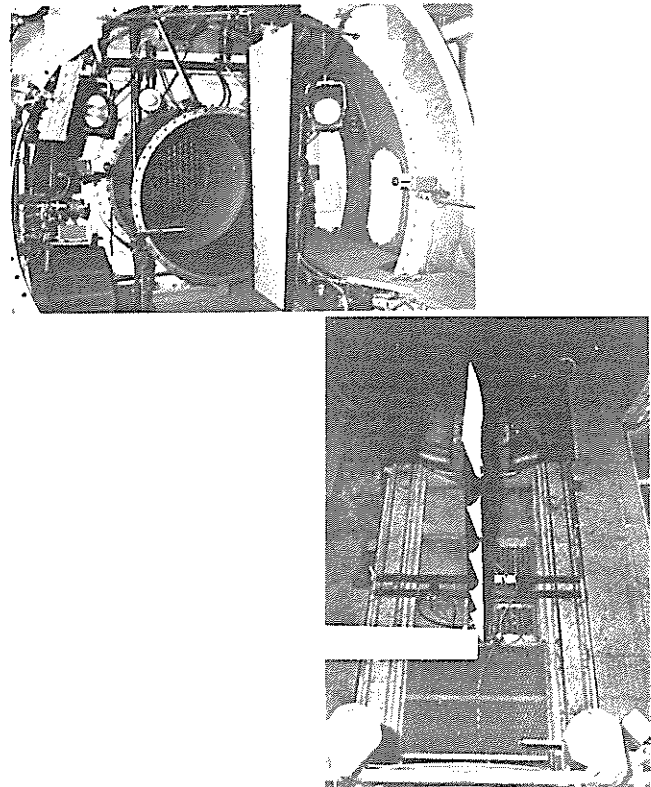


Fig. 21 : HORIZONTAL STABILIZER DEICING TEST SET-UP AT THE CEP_r

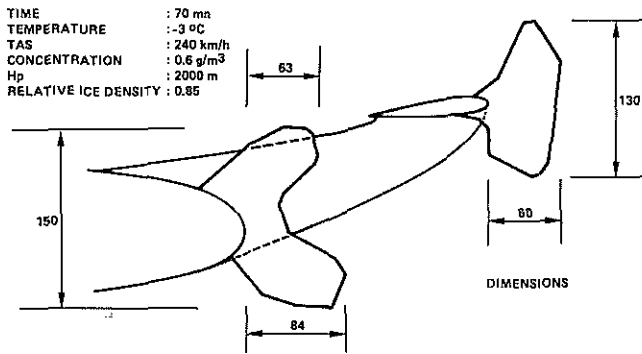


Fig. 22 : HORIZONTAL STABILIZER ICE BUILD-UP OBTAINED FROM ICING TUNNEL TESTS

The pneumatic deicer was dimensioned from accretion tests and was developed entirely in an icing wind tunnel.

The tests carried out are given in Figure 23. The parameters used for the test cover the aircraft flight envelope for speed and incidence (level flight, climb and descent), and the icing envelope given in FAR 25, appendix C

CONFIGURATION	INCIDENCE (°)	AIR SPEED (km/h)	ALTITUDE (m)	DROPLET DIA (μm)	OAT (°C)	LWC (g/m ³)	DURATION (minutes)					
LEVEL FLIGHT	0	250	2000	20	-5	0.7 CMI	17					
						2.35 IMI	15.5					
					-10	0.6 CMI	31					
						2.2 IMI	16.5					
					-20	0.3 CMI	31					
						1.7 IMI	19					
					-30	0.2 CMI	31					
						0.3 CMI	31					
					CLIMB	25	120	2000	20	-5	0.7 CMI	10.5
											2.35 IMI	11
-10	0.6 CMI	16										
	2.2 IMI	11										
-20	0.3 CMI	5										
	1.7 IMI	10.5										
-30	0.2 CMI	10.5										

IMI: FLYING THROUGH A 5 km CLOUD (FAR 25 C, INTERMITTENT ICING) FOLLOWED BY A 5 km FLIGHT THROUGH CLEAR SKY
 CMI: CONTINUOUS MAXIMUM ICING

Fig. 23 : HORIZONTAL STABILIZER DEICING SUBTANTIATION TESTS AT THE CEPR

The tests showed that there was no measurable chordwise accretion outside the protected zone (on the stabilizer and on the slat) except on the spacers (Figure 24).

For all tests, inflation occurs for 6 seconds every 5 minutes. The thickness of residual ice in all cases was less than 10 mm and was acceptable.

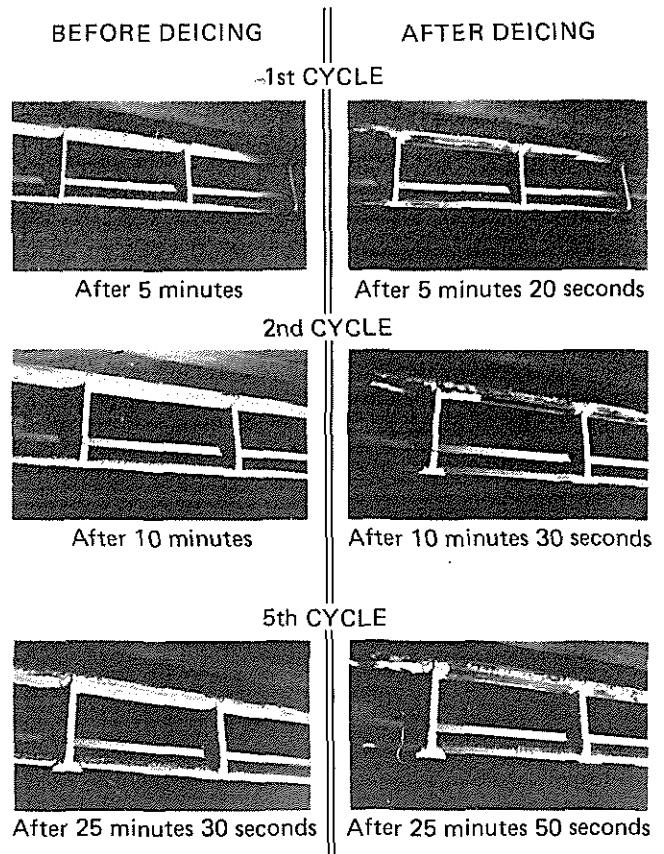


Fig. 24 : HORIZONTAL STABILIZER DEICING SEQUENCES

5 - FLIGHT TESTS IN NATURAL ICING CONDITIONS

Tests were devoted for the main part to finding the most varied natural icing conditions. Correct operation of the icing protection system was checked mainly in cruising flight and every other configuration (climb, descent, approach and go-around, engine failure simulation, etc ..) once these conditions had been found. Aircraft behaviour in the event of a total or partial icing protection system failure was predicted. The above tests were carried out at all-up weight.

Main rotor deicing proved effective in every icing condition encountered. The ice build-ups were measured in negative ground temperature after the flights and refreezing traces were particularly checked for on the blades. Apart from cyclic torque variations associated to the main rotor blades deicing cycle, no significant mean torque change was observed during the longest flight periods in icing conditions (1 hr 50 mn).

The deicing system was substantiated with flight tests from 1981 to 1983 i.e. 53 hours in icing conditions including 12 hours without blade deicing (Figure 25).

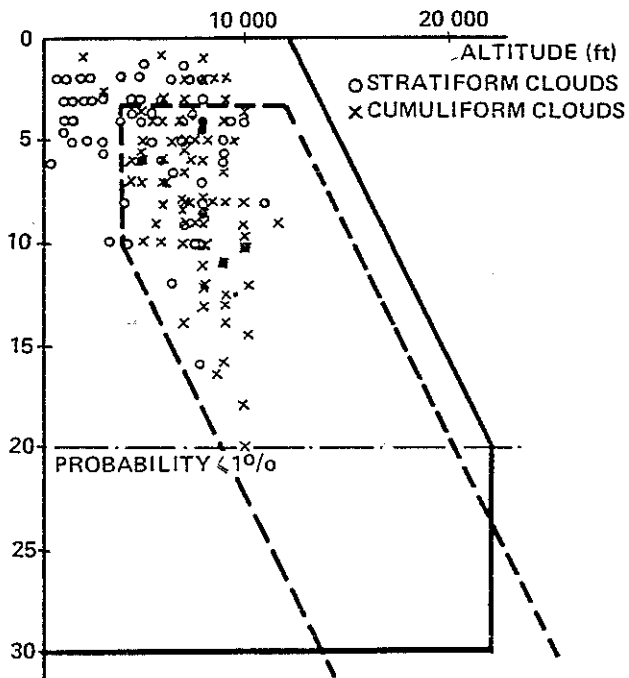


Fig. 25 : ICING CONDITIONS ENCOUNTERED

Results are summarized below :

PARAMETER	MEASURING PROCEDURE	EXTREME VALUES
TEMPERATURE	REVERSE FLUX PROBE	- 20° C
LWC	CEVT 6100 FIXED INDICATOR LEIGH AND ROSEMOUNT PROBES JOHNSON-WILLIAMS HOT WIRE PROBE	2.5 g/m ³ , INTERMITTENT 0.7 g/m ³ , CONTINUOUS
DROPLET DIA.	KNOLLENBERG FSSP	11.5 to 30.5 μ
ALTITUDE		12 000 ft

The main influence of icing on vibrations is a temporary deterioration at 4 Ω p as the blade deicing system goes off ; these transient vibration increases were considered acceptable in every icing condition.

Disymmetric natural icing sometimes produces irregular vibrations as a deicing nozzle failure is simulated ; this irregularity is aggravated, mainly at low temperatures, as the main rotor's deicing system fails completely.

The most significant engine parameter variations were noted in intermittent icing conditions where icing effects may be amplified by turbulence, thus reaching maximum continuous power for a short period of time.

Depending on icing severity, speed in continuous icing conditions is reduced by 5 to 10 kt as an average.

Engine rating is increased to recover the original power upon partial air inlet clogging. Power losses rated 7 % in the most severe flight clogging occurrences.

Flight in icing conditions did not affect handling qualities. The average flight control positions remained unchanged.

6 - CONCLUSION

The efficiency of the Super-Puma icing protection systems has been demonstrated throughout the flight envelope, for the icing conditions specified in FAR 25, Appendix C.

A large part of this demonstration is based on flights in natural icing conditions.

The most critical icing conditions were not necessarily encountered in flight, the demonstration of efficiency constituted a large part of the analysis, primarily for the main rotor and tail rotor blades.

The geometrical dimensioning of the blade protection systems is substantiated by droplet trajectory calculations for the most critical local speed and incidence conditions on the blades, in conjunction with the most critical icing conditions. These calculation methods were validated by confirmation with the airfoil tests in an icing wind tunnel.

The deicing system efficiency demonstration calls for uni- and bi-dimensional methods, which as based on different assumptions lead to the same conclusions : i.e. sufficient blade heating throughout the claimed temperature range (0 to - 30° C in icing conditions), with no risk of re-freezing aft of the protected areas.

In a more conventional manner, the air intake and horizontal stabilizer protection systems were substantiated in an icing wind tunnel and their operation checked in flight in natural icing conditions throughout the envelope explored.

Therefore, on the basis of all these substantiations flight in natural icing conditions, simulated icing in a wind tunnel and analysis the Super-Puma fitted with protective systems obtained DGAC certification in June 1983 and FAA certification in March 1984 for flight in icing atmosphere without limitations.

REFERENCES

- 1 - ADS 4 - FAA - Mars 1964
- 2 - Protection systems against icing on the PUMA
J.C. LECOUTRE
Icing Symposium - London 1978
- 3 - AGARD Advisory report 166
Rotorcraft status and prospects - 1981
- 4 - Aerospatiale's experience on helicopter flight in icing conditions
D. TRIVIER - G. AVEDISSIAN
9th European Rotorcraft Forum - Stresa (Italy) 1983
- 5 - Wind tunnel study of icing and deicing on oscillating rotor blades
G. GUFFOND
8th European Rotorcraft Forum - Aix-en-Provence (France) 1982 (ONERA TP No. 1982 - 116)
- 6 - Overview on icing research at ONERA
GUFFOND - CASSAING - BRUNET
23th AIAA Aerospace Science Meeting - Reno (Nevada) 14-17 January 1985 (ONERA TP No. 1985-4).